Wieczorek, S., Simpson, T. B., Krauskopf, B., & Lenstra, D. (2002). Complex dynamics of an optically injected semiconductor laser : bifurcation theory and experiment.

Complex dynamics of an optically injected semiconductor laser: bifurcation theory and experiment

Sebastian Wieczorek [a], Thomas B. Simpson [b], Bernd Krauskopf [c] and Daan Lenstra [a]

[a]Department of Physics and Astronomy, Vrije Universiteit Amsterdam, De Boelelaan 1081, 1081 HV Amsterdam, The Netherlands

[b]Jaycor, 3394 Carmel Mountain Road, San Diego, CA 92121, USA

[c]Dept of Engineering Mathematics, University of Bristol, Bristol BS8 1TR, UK

ABSTRACT

In this paper unprecedented agreement is reported between a theoretical two-dimensional bifurcation diagram and the corresponding experimental stability map of an optically injected semiconductor laser over a large range of relevant injection parameter values. The bifurcation diagram encompasses both local and global bifurcations mapping out regions of regular, chaotic and multistable behavior in considerable detail.

Keywords: Laser with optical injection, bifurcation diagram.

1. INTRODUCTION

Because the ultimate goal of modeling is to achieve good agreement between theoretical predictions and experimental data we now want to compare our earlier discoveries[1] with the real laser experiment. Earlier quantitative comparisons between experimental data and the single-mode rate equations[2–4] concentrated on spectra for selected bifurcation transitions. We demonstrate here, for a semiconductor laser with optical injection, excellent agreement between theory and experiment on the level of a detailed two-dimensional stability diagram. Our results constitute the first such complete verification of a model of a semiconductor laser system in terms of its complex nonlinear dynamics.

We describe the optically injected laser with three-dimensional rate equations[1] for the slowly varying complex electric field $E = E_x + iE_y$ and normalized inversion n as:

$$\begin{aligned} \dot{E} &= K + \left(\frac{1}{2}(1+i\alpha)n - i\omega\right)E \\ \dot{n} &= -2\Gamma n - (1+2Bn)(|E|^2 - 1)\ . \end{aligned} \tag{1}$$

Eqs. (1) are formulated with respect to the injected optical frequency. There are five parameters appearing in Eqs. (1), of which the injected field strength K and the detuning of the injected field from the solitary laser frequency ω are most important because they can be changed during an experiment. On the other hand, the parameters α, B and Γ are fixed during an experiment as they are given by the material properties of the laser.

As we have shown in our earlier work[1,5–8], system (1) produces a wealth of dynamical complexity, whose systematic investigation is still being continued. In particular, Ref.(1) shows that these results are in good qualitative agreement with an existing experimental stability map[11] obtained by Simpson et al. However, the Fabry-Perot laser used in that experiment showed mode hopping between different longitudinal modes in quite large regions, particularly near the locking boundary for negative detunings. Therefore, a new experiment was proposed; see also Ref.(9). We remark

Further author information (Email addresses) –
S.W.: sebek@nat.vu.nl
T.B.S.: tsimpson@jaycor.com
B.K.: B.Krauskopf@bristol.ac.uk
D.L.: lenstra@nat.vu.nl

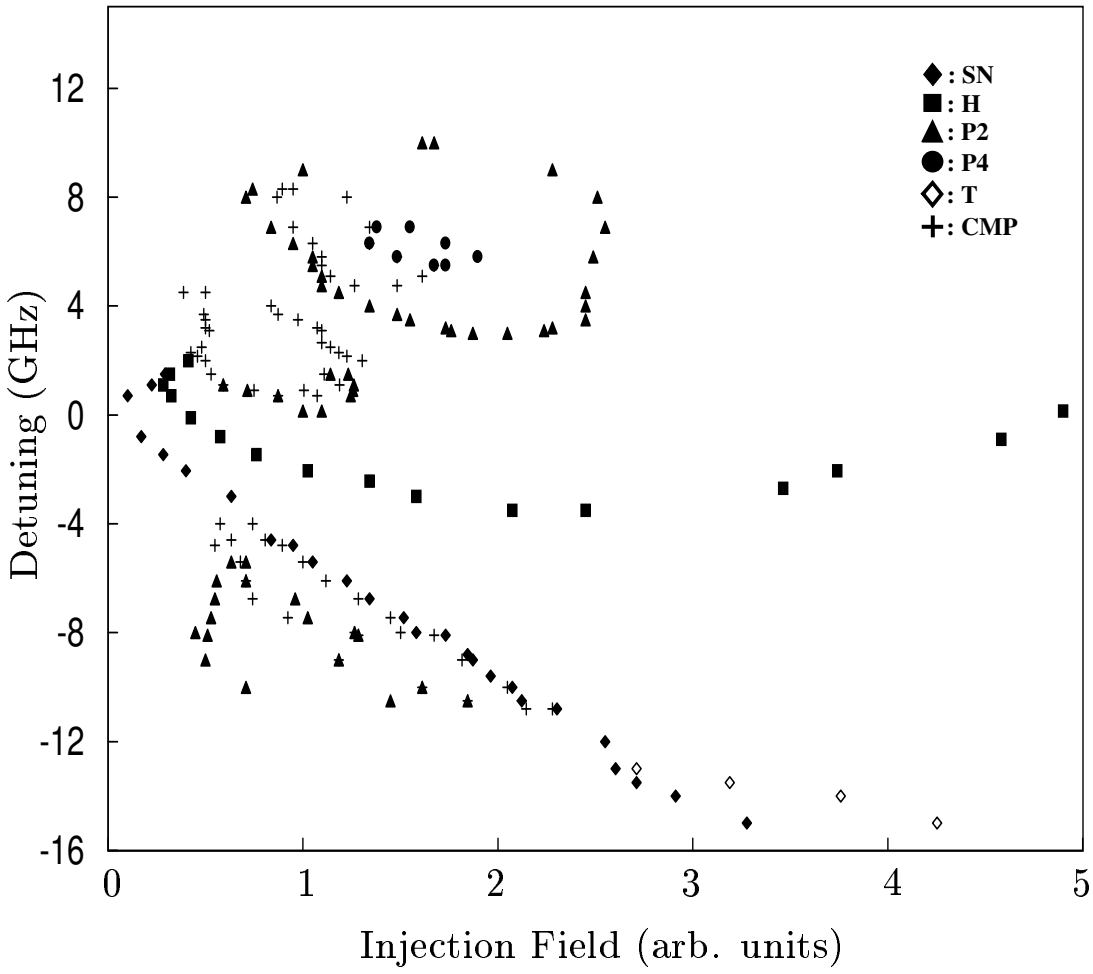

Fig. 1. Experimental bifurcation diagram.

that recently similar experiments with a Fabry-Perot laser, also showing mode hopping in certain regions, have been obtained in Ref.(12) by extensive sweeps of injected light for different detunings.

Our main result is presented in two bifurcation diagrams: one obtained for a DFB-semiconductor laser operating at 1.557 μm, which is strictly single-mode throughout the entire range of injection values (Fig. 1), and a theoretical bifurcation diagram for this DFB laser computed with numerical continuation methods (Fig. 2). These results were not obtained separately. The experimental measurements were guided by the theoretical predictions leading to experimental identification of extra phenomena, such as a bistability and a chaotic intermittent transition. Indeed, the agreement between theory and experiment is so good that quantitative prediction of complex laser dynamics is possible.

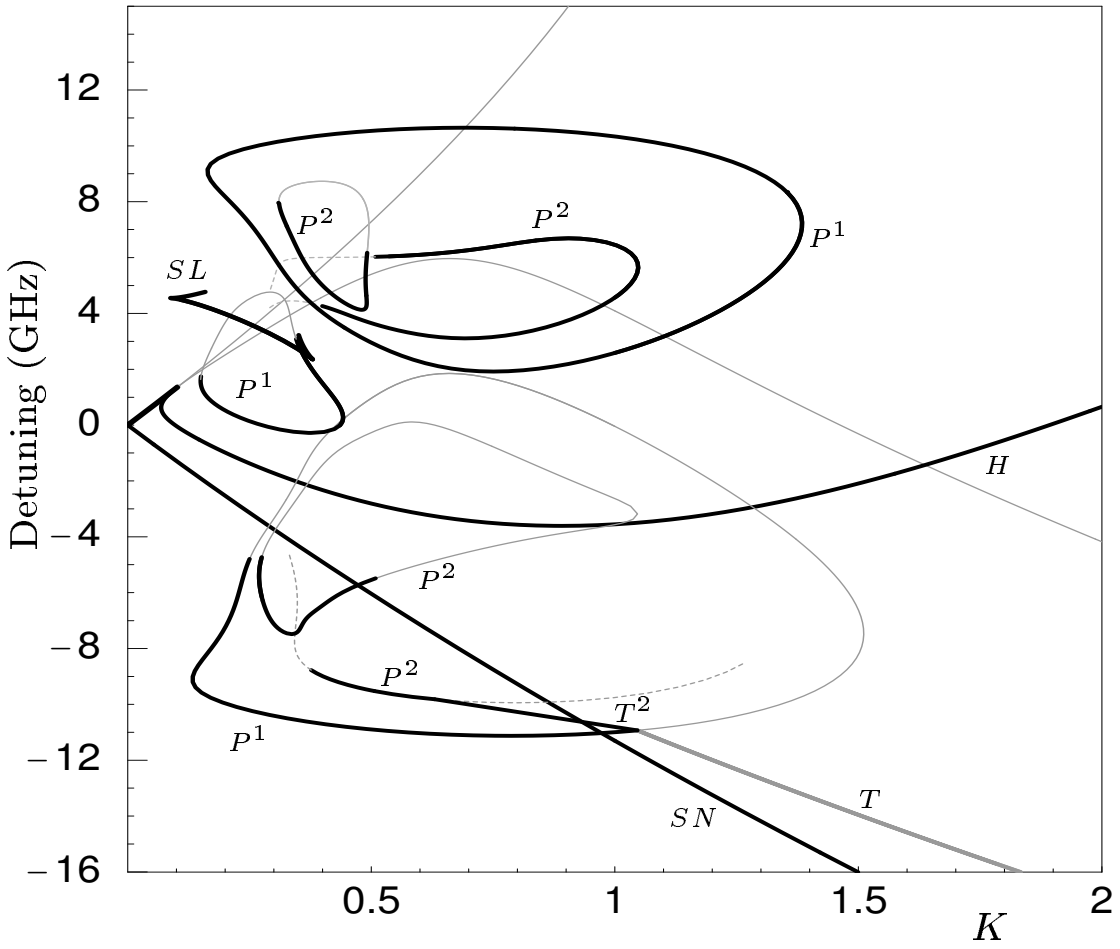

Fig. 2. Theoretical bifurcation diagram of Eqs. (1).

2. BIFURCATION THEORY AND LASER EXPERIMENT

The curves in Fig. 2 are computed from (1) for the experimentally obtained parameter values $\alpha = 2.6$, $B = 0.0295$ and $\Gamma = 0.0973$ specifying the DFB laser used in the experiment. Specifically, α was determined by measuring the asymmetry of the modulation sidebands in the optical spectra of the DFB laser subject to weak current modulation[13], while B and Γ were determined from measurements of the amplitude (output power) spectra of the laser subject to weak optical injection[14]. For the operating conditions of Fig. 2, $\Gamma_0 \approx 5 \cdot 10^{11}$ s^{-1}, $\Gamma_N \approx 4 \cdot 10^9$ s^{-1} and $\omega_R \approx 29.5 \cdot 10^9$ rad/s. The error estimate for α is approximately -15% to $+10\%$, while for the other parameters it is less than $\pm 10\%$. Each curve in Fig. 2 corresponds to a specific bifurcation and they all fit together on a global level into a consistent structure that divides the $(K, \omega)-$plane into regions of different types of laser output. In Fig. 2, SN denotes saddle-node bifurcation of equilibria, H denotes Hopf bifurcation, P denotes period-doubling bifurcation, T denotes torus bifurcation, and SL denotes saddle-node of limit cycle bifurcation; superscripts say what the period of the bifurcating limit cycle is. Supercritical bifurcations are plotted as black curves, and subcritical bifurcations are plotted as gray curves. See Ref.(10) as a general reference to bifurcation theory.

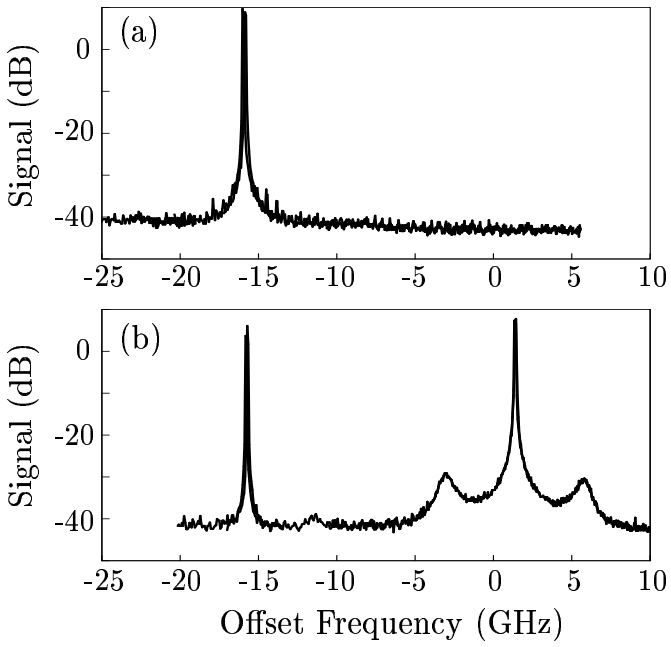

Fig. 3. Experimental spectra of the stable equilibrium (a) and periodic orbit (b). Each plot shows two traces of the spectrum; $\omega = -16$ GHz and the Injection Field was ≈ 3.5.

Recall that Eqs. (1) are written in the reference frame where the injected field has zero frequency. On the other hand, the 'Offset Frequency' appearing in figures of spectra is given with respect to the solitary laser frequency.

The new experimental results are shown in Fig. 1. For the DFB-semiconductor laser that was used, less than 1% (measurement uncertainty) of the total output power was contained in the side modes. Further, under optical injection the power in the side modes deviated by less than 10% from its free-running value over the range of operating conditions studied. The fiber-coupled experimental apparatus consists of an optically isolated master laser that is coupled to the slave laser through a variable attenuator and an optical circulator. Both master and slave laser are under independent current and temperature control. The slave laser was biased at twice its lasing threshold, and its output is mixed with the frequency-tunable output from a third laser that acts as a local oscillator and then detected by a photodiode. As the local oscillator's optical frequency is tuned across the range of optical frequencies generated by the slave laser, the optical spectrum is measured using a microwave spectrum analyzer. Frequency resolution is better than 100 MHz and the dynamic range is greater than 50 dB. Optical spectra, like those shown below, are used to identify operating conditions where stable, periodic, and more complex operating characteristics are observed[2,11]. The offset frequency of the master laser with respect to the slave laser is adjusted by changing its operating temperature. The injected power is adjusted by changing the variable attenuator. An experimental bifurcation diagram is generated by stepping the master laser through operating points of interest and recording the optical spectra generated by the slave laser under optical injection.

In Figure 1 each symbol indicates an observed qualitative change of spectral characteristic. Full diamonds correspond to the transition from stable, locked operation to unlocked operation while the open diamonds at large negative offset frequencies correspond to the transition from unlocked to stable locked operation. Squares denote the appearance of the relaxation oscillation. Triangles bound regions of period-two operation, circles confine regions of period-four oscillation and crosses bound regions of more complicated spectral and dynamic characteristics. Small pockets of periodic dynamics in these regions are not shown. To absolutely compare model and experiment it would be necessary to measure the power from the master laser that is actually coupled into the oscillating mode of the slave laser, not simply measure the power incident on the laser facet. Because this was not possible, we used the experimentally observed locking-unlocking transition and the calculated saddle-node curve as the calibration reference.

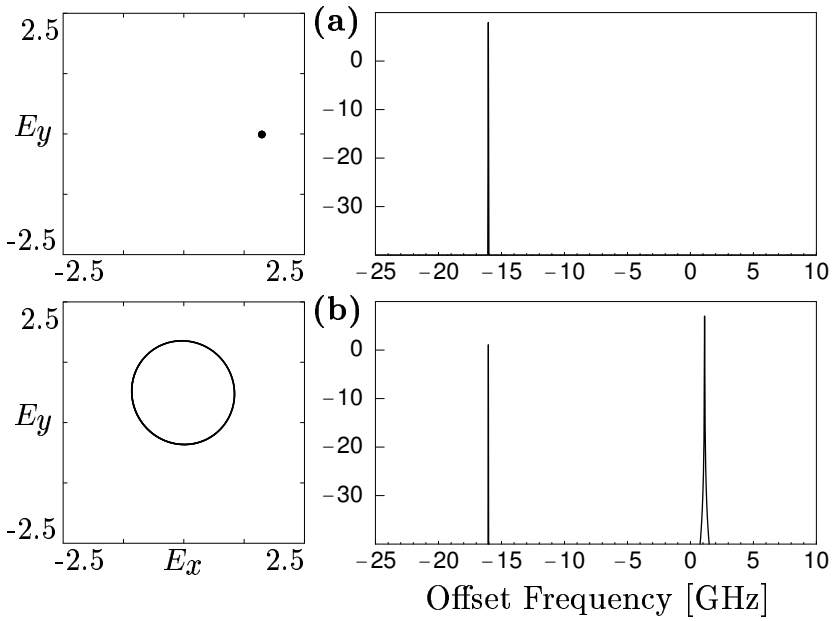

Fig. 4. Phase portraits (left column) and spectra (right column) of Eqs. (1) of the two coexisting stable states, an equilibrium (a) and periodic orbit (b); $\omega = -16$ GHz and $K = 1.7$.

Clearly, several curves in Fig. 2 show very good agreement with the respective measurements in Fig. 1 within a few percent, while particularly in the upper region bounded by period-doublings the agreement is less spectacular, but still on the order of about 25 percent. This may seem much but in the field of dynamical systems it is an extraordinary achievement. While the bifurcation diagram comprises many different physical phenomena which depend on different parameters that are often difficult to estimate accurately, the agreement is well within the accuracy of the experimental determination of the laser parameters. This is why we claim that Figures 1 and 2 demonstrate overall quantitative agreement between theory and experiment. Furthermore, the agreement is so good that it allows for quantitative predictions of complex dynamics.

We now discuss the general structure of Figs. 1 and 2 in more detail. In the locking region, confined between the two curves SN and H in Fig. 2, the laser emits light exactly at the frequency of the injected light. As the locking region is approached from below for $K < 1$, the slave laser emits an oscillating signal (due to the beating between the master and slave fields) until SN is reached where a stable equilibrium appears in a saddle-node bifurcation (for $K > 1$ there is a bistability discussed hereafter). Between SN and H the slave laser locks to the injected field. Along curve H, the stable equilibrium loses its stability in a Hopf bifurcation, and a sustained relaxation oscillation is found above H. A periodic orbit, of 'basic' period $\approx 2\pi/\omega_R$ at low injection levels and monotonically decreasing period at higher injection levels, then appears and the laser produces a stable intensity oscillation.

Periodic solutions may encounter further instabilities. Figure 2 shows three regions bounded by period-doubling bifurcations P^1 of the basic periodic orbit, one for negative detuning ω, and a small and a bigger region for positive ω. Transitions from period-two to period-four operation occur along the curves P^2.

The period-doubling curves for negative ω agree well with the measurements, to within a few percent. Furthermore, the crosses, signaling a change to chaotic dynamics in the measured spectra, agree very well with the theoretical boundary of complicated dynamics given by the accumulation of period-doubling curves and the locking range[5]. Where the lower period-doubling curve P^1 changes from super- to subcritical a curve of torus bifurcations emerges, leading to quasiperiodic or synchronized oscillations, depending on the ratio of the two frequencies involved. The attracting torus born along the black curve T^2 breaks up into a chaotic attractor[6] and this leads to the chaotic dynamics above T^2 detected experimentally in this region (crosses). The gray torus bifurcation curve T, on the other hand, bounds a region of bistability, discussed in Ref.(5), between the running phase solution and the locked solution.

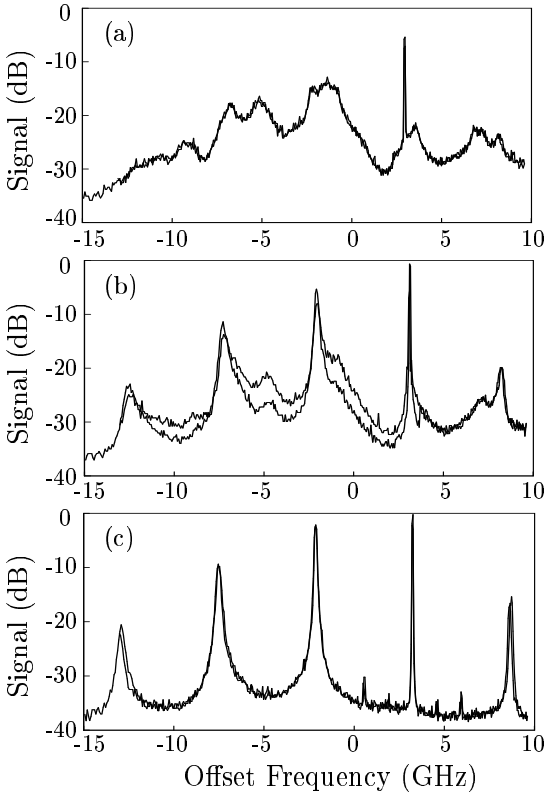

Fig. 5. Experimental spectra showing an intermittent transition. Each plot shows two traces of the spectrum; the Injection Field was ≈ 1 and ω from (a) to (c) takes the values 3, 3.13, and 3.2 GHz.

The bistability phenomenon was observed in Ref.(15) and then it was studied numerically in Ref.(16) but the authors did not recognize the underlying bifurcation mechanism. This motivated the asymptotic analysis which revealed the existence of the torus bifurcation curve for negative detunings[17]. The bistability region opens at ≈ -12 GHz and its other boundary is SN. The upper bistability boundary was found experimentally (open diamonds) to within a few percent of the theoretical curve T. At low injection, the laser settles down to a periodic orbit (the running phase solution). By injecting more light, a stable equilibrium appears on the black part of SN. The two attractors coexist as shown in Figs. 4 and 3, but the equilibrium is unnoticed until the gray curve T is crossed. Then the stable periodic orbit becomes unstable via a subcritical torus bifurcation (T in Fig. 2 and open diamonds in Fig. 1) and all trajectories converge to the stable equilibrium. In the opposite direction, the stable periodic orbit appears on T and remains unnoticed until SN. This completes the hysteresis loop associated with this bistability[15]. Sidebands around the right-hand, unlocked peak of Fig. 3 are the noise-induced, damped relaxation oscillation, and similar, but weaker, features appear in the spectrum of the free-running laser[11]. This region of bistability was not found in the Fabry-Perot laser used in Ref.(11) due to mode hopping in this region of the (K, ω)-plane.

Bifurcation curves from Fig. 2 form the backbone of the injected laser dynamics but there exist more bifurcations describing new effects. However, computing more and more detail raises the classical modeling question: are the transitions we calculate still relevant for the real system under consideration? In fact, the excellent agreement between the model and the real laser obtained so far also extends to the level of complicated global bifurcations. We demonstrate this with an intermittent transition out of chaos.

For the small central region of period-doubling and complex dynamics the agreement between theory and experiment is good, to within 10%. Again, the triangles and crosses agree well with the region bounded by the theoretical bifurcation curves. The chaotic region inside the curves P^1 and P^2 can be entered (or exited) in different manners, and one is an intermittent transition from periodic oscillations directly to chaos caused by a global saddle-node of periodic orbit bifurcation taking place on a chaotic attractor[8]. This transition is explained in detail in Ref.(8) and happens along the black curve SL. Experimentally, this chaotic region is confined from above by crosses, already

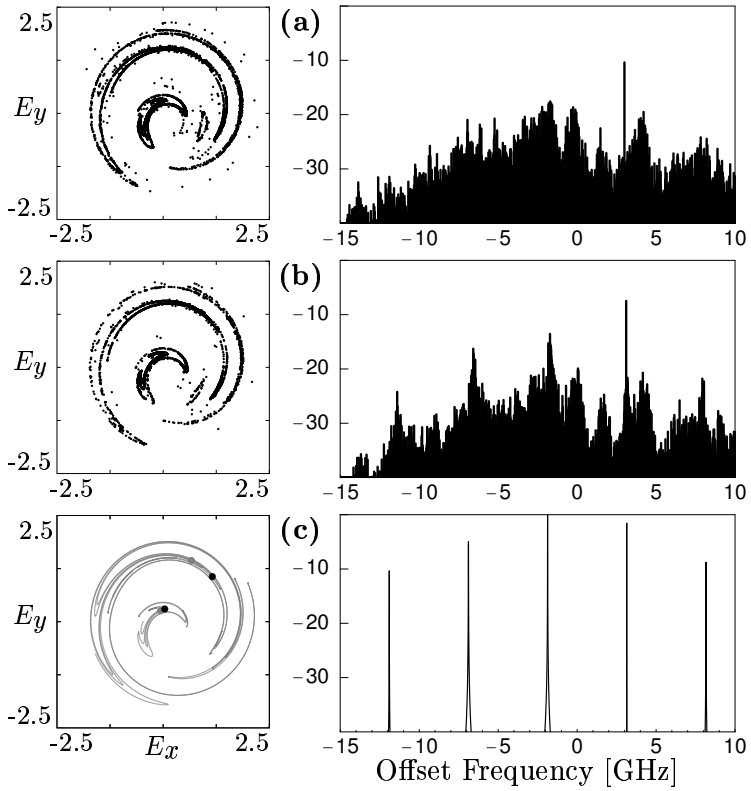

Fig. 6. Intermittent transition in Eqs. (1). Shown are attractors in the Poincaré section $\{n = 0\}$ (left column) and the corresponding spectra (right column); $K = 0.31$ and ω from (a) to (c) takes the values 3, 3.11, and 3.15 GHz.

suggesting an abrupt transition out of chaos. Detailed measurements of spectra in this region, shown in Fig. 5, reveal an intermittent transition. The chaotic signal in Fig. 5(a) changes abruptly to oscillations in (c). Very close to the bifurcation value, one sees fluctuations of the spectrum between the two cases due to parameter jitter, as is shown by the two overlaid spectra in Fig. 5 (b). The experimental spectra reveal structures that agree very well with those computed from Eqs. (1), shown in Fig. 6. Notice in Fig. 6(a) and (b) that the chaotic attractor anticipates a periodic orbit that is about to appear, as demonstrated by the development of the narrow equidistant peaks in the spectra. Then, at the saddle-node of periodic orbit bifurcation SL, two new periodic orbits appear, one attracting and one a saddle orbit. The laser makes a sudden transition from chaotic to periodic oscillations in Fig. 6(c). Although the chaotic attractor no longer exists, its structure is still present as is evident from the unstable manifold of the new saddle orbit [the gray structure in the Poincaré section of Fig.6(c)]. An abrupt transition was observed in previous experiments[2,11] but then it was unclear whether the effect was genuine or due to multimode laser operation. This shows the value of bifurcation diagrams as a tool to find and interpret complicated transitions in this laser system.

The deviation between theory and experiment is not exceeding about 25% for the large upper region of period-doubling and complex dynamics. In particular, the crosses indicating transition to complex dynamics are in good agreement with the theoretical prediction. It is unclear why the deviation between model and experiment should be greatest for positive detunings at large injection levels. It is known that α is a critical parameter in determining the nonlinear dynamics. Further, optical injection induces changes in the carrier density and there is some evidence that α may be sensitive to the changes[13]. Indeed, the model rests on the fact that the complex gain can be linearly related to the carrier density, spatially averaged over the laser structure. It is extraordinary how well this simplification holds for this laser, given the variations in the optical field and carrier density over the structure.

3.CONCLUSIONS

In conclusion, for the nonlinear dynamical behavior of a semiconductor laser with optical injection we have presented a comparison between an experiment using a single-mode DFB semiconductor laser and bifurcation theory based on Eqs. (1). Very good agreement, not only locally but also globally, has been obtained in unprecedented detail. Furthermore, we have used the model to make quantitative predictions about details of the nonlinear dynamics, specifically determining the detuning and injection levels required for the bistability, and the mechanism and characteristics of an intermittent transition to chaos. This demonstrates predictive and quantitative modeling of nonlinear laser dynamics, and it constitutes the state of the art in dynamical systems modeling of a complex system.

From an application point of view, the mapping out of dynamics in its full global context, opens exciting new possibilities for applying a single device to all-optical signal manipulation.

ACKNOWLEDGEMENTS

The research of S.W. was supported by the Foundation for Fundamental Research on Matter (FOM), which is financially supported by the Netherlands Organization for Scientific Research (NWO). The work of T.B.S. was supported, in part, by the U.S. Army Research Office under contract DAAG-55-98-C-0038.

REFERENCES

1. S. Wieczorek, B. Krauskopf and D. Lenstra "A unifying view of bifurcations in a semiconductor laser subject to optical injection", *Opt. Comm.* **4172**(1-6) (1999) 279–295.
2. V. Kovanis, A. Gavrielides, T.B. Simpson, and J.M. Liu, "Instabilities and chaos in optically injected semiconductor lasers", *Appl. Phys. Lett.* **67** (19) (1995) 2780–2782.
3. T.B. Simpson, J.M. Liu, A. Gavrielides, V. Kovanis, and P.M. Alsing, "Period-doubling route to chaos in a semiconductor laser subject to optical injection", *Appl. Phys. Lett.* **64** (26) (1994) 3539–3541.
4. T.B. Simpson, J.M. Liu, A. Gavrielides, V. Kovanis, and P.M. Alsing, "Period-doubling cascade and chaos in a semiconductor lasers with optical injection", *Phys. Rev. A* **51** (5) (1995) 4181–4185.
5. S. Wieczorek, B. Krauskopf and D. Lenstra, "Mechanisms for multistability in a semiconductor laser with optical injection", *Opt. Comm.* **183**(1-4) (2000) 215–226.
6. B. Krauskopf, S. Wieczorek, and D. Lenstra, "Different types of chaos in an optically injected semiconductor laser" *Appl. Phys. Lett.* **77** (11) (2000) 1611–1613.
7. S. Wieczorek, B. Krauskopf, and D. Lenstra, "Sudden chaotic transitions in semiconductor laser with optical injection.", *Opt. Lett.* **26**(11) (2001) 816–818.
8. S. Wieczorek, B. Krauskopf, and D. Lenstra, "Unnested islands of period-dublings in an injected semiconductor laser", *Phys. Rev. E* **64** 056204 (2001) 1–9.
9. S. Wieczorek, T.B. Simpson, B. Krauskopf, and D. Lenstra, "Global quantitative predictions of complex laser dynamics", *Phys. Rev. E*, to appear in April 2002.
10. Yu.A. Kuznetsov, *Elements of Applied Bifurcation Theory*, Applied Mathematical Sciences **112**, Springer 1995.
11. T.B. Simpson, J.M. Liu, K.F. Huang, and K. Tai, "Nonlinear dynamics induced by external optical injection in semiconductor lasers", *Quant. Semiclass. Opt.* **9** (5) (1997) 765–784.
12. S. Eriksson and Å. M. Lindberg, "Observations on the dynamics of semiconductor lasers subjected to external optical injection", *submitted* (2002).
13. T.B. Simpson, F. Doft, E. Strzelecka, J.J. Liu, W. Chang, and G.J. Simonis, "Gain saturation and the linewidth enhancement factor in semiconductor lasers", *IEEE Photon. Technol. Lett.* **13** (8) (2001) 776.
14. J.M. Liu and T.B. Simpson, "Four-wave mixing and optical modulation in a semiconductor lasers", *IEEE J. Quantum Electron.* **30** (4) (1994) 957.
15. R. Hui, A. D'Ottavi, A. Mecozzi, and P. Spano, "Injection locking in distributed feedback semiconductor lasers" *IEEE J. Quantum Electron.* **27** (1991) 1688.
16. J.M. Liu, H.F. Chen, X.J. Meng, and T.B. Simpson, "Modulation bandwidth, noise, and stability of a semiconductor laser subject to strong injection locking", *IEEE Photon. Techn. Lett.* **9** (1997) 1325.
17. V. Kovanis, T. Erneux, and A. Gavrielides, "Largely detuned injection-locked semiconductor lasers", *Opt. Comm.* **159** (1999) 177–183.